Functional characterization of correct and incorrect feature integration

Pablo Rodríguez-San Esteban[1*], Ana B. Chica[1*] & Pedro M. Paz-Alonso[2,3]

[1] Department of Experiment Psychology and Brain, Mind and Behavior Research Center (CIMCYC), Universidad de Granada, España

[2] BCBL, Basque Center on Cognition, Brain, and Language, Donostia, España

[3] IKERBASQUE, Basque Foundation for Science, Bilbao, España

*These two authors have contributed equally to this work

ORCID numbers:

Pablo Rodríguez-San Esteban: 0000-0003-2020-9015

Ana B. Chica: 0000-0001-5804-1591

Pedro M. Paz-Alonso: 0000-0002-0325-9304

Correspondence should be addressed to Ana B. Chica, Department of Experimental Psychology, Faculty of Psychology, 18071, Granada, Spain. Phone number: +34 958247879. Fax number: +34 958246239 Email: anachica@ugr.es

Total number of words: 6515

Running title: Functional characterization of feature integration.

Highlights

- Our results underscore the critical role of the parietal cortex in feature integration.
- Correct feature integration is characterized by increased occipito-parietal functional connectivity.
- Incorrect feature integration is characterized by increased activation of occipital areas at earlier time points, reduced right occipital-FEF coactivation at later time points, and overall decreased occipito-parietal coactivation.

Abstract

Our sensory system constantly receives information from the environment and our own body. Despite our impression to the contrary, we remain largely unaware of this information and often cannot report it correctly. While perceptual processing does not require conscious effort on the part of the observer, it is often complex, giving rise to errors such as incorrect integration of features (illusory conjunctions). In the present study, we use functional magnetic resonance imaging to study the neural bases of feature integration in a dual task that produced around 30% illusions. A distributed set of regions demonstrated increased activity for correct compared to incorrect (illusory) feature integration, with increased functional coupling between occipital and parietal regions. By contrast, incorrect feature integration (illusions) was associated with increased occipital (V1-V2) responses at early stages, reduced functional connectivity between right occipital regions and the FEF at later stages, and an overall decrease in coactivation between occipital and parietal regions. These results underscore the role of parietal regions in feature integration and highlight the relevance of functional occipito-frontal interactions in perceptual processing.

Keywords: Feature Integration, Functional Connectivity, Illusory Conjunctions.

Introduction

At any given moment, the central nervous system receives a vast amount of information through the senses. Although we subjectively believe that we perceive most of this information, we are only capable of consciously reporting a small fraction of it. This underscores the difference between the large amounts of information that are (at least partially) represented in "phenomenal consciousness" (Block 1995, 2011) and the limitations of "access consciousness". While perceptual processes do not entail conscious effort on the part of the observer, several aspects of perception are computationally complex, for instance, processing a set of features (e.g., color, form, size, etc.) and integrating them to construct a single percept (Treisman 1998). This perceptual integration has been related to phenomenal consciousness (Block 2005; Lamme 2010). Both processes are highly related since both reflect the unified and holistic nature of conscious experience (Mudrik et al. 2014). It has been proposed that integration is necessary for conscious experience and that conscious experience is necessary for the integration of information coming from different networks, supported by long-range connections (Lamme 2006).

Attention has been related to both access and phenomenal consciousness (Chica and Bartolomeo 2012; Pitts et al. 2018). In accordance with the Feature Integration Theory (FIT) proposed by Treisman and Gelade (1980), attention is necessary for the correct integration of features (although, see Fahrenfort et al. 2017, Discussion section). Without attention, features might be erroneously combined (Treisman 1998). When integration processes fail, they result in "illusory conjunctions", an erroneous perception in which two features from distinct elements are conjoined to produce a single, specific configuration (Treisman and Schmidt 1982). The likelihood of a binding failure increases in the absence of attention and can lead to illusory conjunctions (Treisman and Schmidt 1982). Thus, dual tasks and brief stimulus presentations are associated with a larger percentage of illusory conjunctions (Treisman and Gelade 1980). These results support the idea that such illusions result from limitations in attentional resources (Humphreys 2016), perhaps due to excessive cognitive load (Treisman and Schmidt 1982).

An alternative model, the Feature Confirmation Account (FCA), claims that while attention is important, it is not critical for feature integration, that is, establishing stable representations through top-down matching of rich but unstable input data (Humphreys 2016). It was proposed that feature relations could be coded at the early stages of visual processing in the striate or extrastriate cortex, based on the presence of a limited set of conjunctive relations between neurons in these regions (Treisman 1998; Li 2002). Gillebert and Humphreys (2010) proposed a two-stage account of feature integration, with an initial bottom-up stage of feature integration based on the activation of neurons sensitive to conjunctions of visual features. Subsequently, however, there is a slow process in which the results of the initial stage are confirmed through top-down feedback (the process of attentional confirmation). This slow confirmation process is supported by the parietal cortex (Humphreys 2016; see Braet and Humphreys 2009). Therefore, according to the FCA, feature conjunctions are coded early on in visual processing, but they are noisy and relatively transient unless supported by top-down feedback from the posterior parietal cortex. This hypothesis proposes an initial bottom-up stage of feature integration based on the activation of neurons sensitive to visual feature conjunction, which is subsequently confirmed through top-down feedback from the parietal cortex (Braet and Humphreys 2009; Gillebert and Humphreys 2010; Humphreys 2016).

Neuropsychological evidence from early studies suggests that illusory conjunction rates rise after brain lesions which damage bilateral parietal and parieto-occipital (Friedman-Hill et al. 1995; Bernstein and Robertson 1998; Robertson 2003), or right parietal cortex (Gillebert and Humphreys 2010). The parietal cortex has been associated with different processes related to visual search and object selection, such as attention, feature binding, and visual working memory (Leonards et al. 2000), as well as spatial information processing (Shafritz et al. 2002). It has been suggested that the parietal lobe influences feature integration because it constitutes a key node for visuo-spatial processing (Fiebelkorn and Kastner 2020).

Several parietal regions (including the intraparietal sulcus [IPS], postcentral sulcus, as well as the superior parietal cortex) and some occipital regions (including the transverse occipital sulcus [TOS]), especially within the right hemisphere, show more activation in tasks that require searching for a conjunction of features rather than single features (Donner et al. 2000; Leonards et al. 2000; Shafritz et al. 2002; Pollmann et al. 2014). Although evidence from non-invasive neurostimulation techniques is still scarce, the role of the parietal cortex in feature binding has also been supported by transcranial magnetic stimulation (TMS) studies, which demonstrated that after stimulation of the right intraparietal sulcus, fewer illusory conjunctions were produced, but the perception of basic features remained unaltered (Esterman et al. 2007). Moreover, TMS over parietal areas can disrupt conjunction search but not feature search (Robertson 2003) and increase the proportion of illusory conjunctions when TMS pulses occur 150 ms after the target, but not before (Braet and Humphreys 2009).

Previous research has also highlighted a role for the parietal cortex in feature integration, although it is unclear whether this role is related to attention (Kastner and Ungerleider 2000; Shafritz et al. 2002) or feature confirmation (Humphreys 2016). One way to further investigate the role of the parietal cortex in feature integration is to explore not only its response to different experimental conditions in isolation, but also its interactions with other brain regions. The present functional magnetic resonance imaging (fMRI) study was aimed at investigating the neural interplay underlying feature integration, exploring the role of the parietal cortex, the frontal eye field (FEF; a region associated with attentional selection; Hung et al. 2011; Ramkumar et al. 2016) and occipital regions by directly comparing correct perception of visual stimuli with illusory conjunctions. Our aim was to explore the neural mechanisms associated with correct and incorrect feature integration, which might provide evidence in regard to the role of the parietal cortex on attention (as proposed by the FIT) or on feature confirmation (as proposed by the FCA). We adapted a paradigm from Esterman and colleagues (Esterman et al. 2004, 2007) that produces illusory conjunctions to study

feature binding in a simultaneous behavioral task that manipulates divided attention at two levels of difficulty (Cobos and Chica 2022).

If, as proposed by the FIT, attention was necessary for feature integration: 1) more illusory conjunctions should be observed in the more demanding, as compared to the less demanding, central task condition; and 2) at the neural level, the same regions demonstrating modulations by the central task demands should also show differential responses to correct and incorrect feature integration trials. Based on the results of previous studies, we predicted that correct responses would be accompanied by stronger activation than illusory conjunctions in attentional regions, such as the right parietal cortex and the right FEF (Donner et al. 2000; Leonards et al. 2000; Shafritz et al. 2002; Baumgartner et al. 2013). We also expected to observe increased functional connectivity between occipital and parietal regions for correct responses compared to illusory conjunctions. The FIT predicts increased parietal cortex activation given increased attentional processes while the FCA predicts increased parietal cortex activation with top-down matching for rich but unstable input data. As for the occipital regions, the FIT predicts that amplified attention from the parietal cortex will increase occipital responses for correct responses, as compared to illusory conjunctions, while the FCA predicts a larger (but unstable) response in occipital regions for illusory conjunctions than correct responses (Braet and Humphreys 2009; Humphreys 2016).

Materials and Methods

Participants

The final study sample included 28 volunteers (16 females, mean age 23.75 ± 3.03 years). Data from 5 additional participants were excluded from further analyses due to excessive head motion during scanning (3 participants) or technical problems during data acquisition (2 participants). All participants were right-handed and had normal or corrected-to-normal vision, normal color perception, and no prior experience with the task. No participant had a history of major medical, neurological, or psychiatric disorders. Participants received a monetary compensation of 10€/h for

their participation. Signed informed consent was collected prior to their inclusion in the study. Participants were informed about their right to withdraw from the experiment at any time. CEIM/CEI Granada's Biomedicine Research Ethics Committee approved the experiment, which was carried out in accordance with the Code of Ethics of the World Medical Association (Declaration of Helsinki) for experiments involving humans.

Apparatus and Stimuli

E-Prime software (version 2.0, Schneider et al. 2002) was used for stimuli presentation and behavioral data collection. Stimuli were presented on a screen (NNL, 32'', 1024 × 768, 60 Hz) located in the control room 2.12 m away from the scanner; participants viewed the presentation through a mirror mounted on the head coil. Behavioral responses were recorded with two horizontally aligned 6-button response pads, connected by optical fiber to an Evoke Response Pad interface box (Resonance Technology INC., http://www.mrivideo.com/).

The task was an adaptation based on Esterman and colleagues (Esterman et al. 2004, 2007) see also Cobos and Chica 2022). First, a number was presented above the fixation cross and remained on the screen until the end of the trial. A string of characters (containing the target letter "L" and some distractors) was then briefly displayed at either the right or the left of the fixation cross, followed by a mask. Participants were required to report if the central number was smaller or greater than 5 (central task), and then to indicate the color of the letter "L" (peripheral task; see Procedure section and Figure 1).

Stimuli consisted of a white cross (0.27º) presented in the center of the screen, functioning as a fixation point. The peripheral stimulus consisted of a horizontal string of four characters (7.55x1.75º) presented either to the right or left of the fixation point. The string was composed of two inner characters, the target letter "L" and the distractor "O", which appeared in two different colors, either red (RGB% 215, 0, 0), blue (RGB% 46, 118, 182) or green (RGB% 0, 135, 61). The two

outer characters were printed in white and could be either “S” or “8”. A mask, comprising four white “&” characters (7.55x1.75º) was also presented after each string of characters.

Before the string of characters appeared, a number was presented in white above (0.27º) the fixation point. This number could take values between 1 and 9, excluding 5. This allowed us to implement the two difficulty conditions in the Central task (see Procedure section), with the more difficult condition comprising “near” numbers 3, 4, 6, 7, and the less difficult condition comprising “far” numbers 1, 2, 8, 9.

Procedure

The sequence of the events in each trial is shown in Figure 1. Each trial began with a fixation point (1000ms). Then, the number was presented and remained on screen for a total duration of 2100ms; 50% “far” and 50% “near” numbers were presented in random order. The character string appeared 300ms after the onset of the number, appearing for 100ms either to the right (50%) or left (50%) of the fixation cross, also in random order. After an interstimulus interval (ISI, 50ms), the mask was displayed for 100ms. As soon as the number was presented, participants responded to the central task using their right hand. They were required to press a button with their index finger if the number was smaller than 5 or another button with their middle finger if it was greater than 5 (the response mapping was counterbalanced across participants). They were asked to provide the response as quickly and accurately as possible while the number remained on the screen, within a temporal window of 1550ms. This task is known to produce faster and more accurate responses for far as compared to near conditions (Cobos and Chica 2022). After the number disappeared, participants were instructed to respond to the peripheral task, using the index, middle, or ring fingers of their left hand to report the color of the letter “L” (red, blue, or green). Color-key mapping was counterbalanced across participants. If they were not aware of the color of the letter “L”, they were instructed to respond with their left thumb. Participants were asked to respond to this task as accurately as possible, within a temporal window of 3100ms. Responses to this peripheral task were

categorized as *hits* when the color of the letter "L" was correctly reported, *illusions* when participants reported the color of the letter "O", *errors* when participants reported a color that was not present in the display, and *unseen* (when participants could not report the color of the letter).

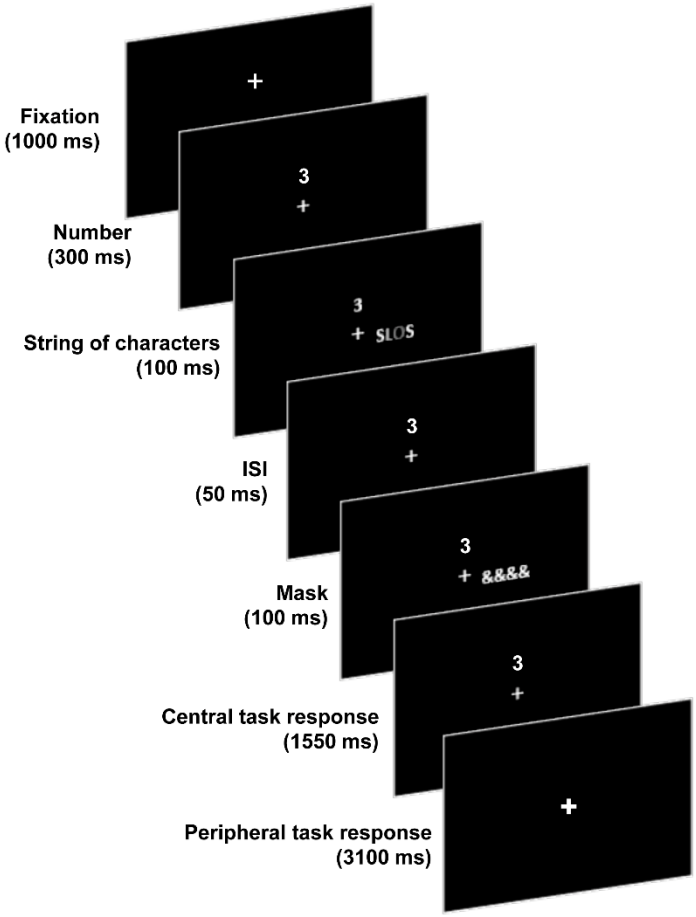

Figure 1. Sequence and timing of trial events. Participants first responded to the central task, reporting if the number was smaller or larger than 5. After providing this speeded response, participants indicated, as accurately as possible, the color of the letter. The string of characters was composed of two inner characters, the target letter "L" and the distractor "O", which appeared in two different colors, either red, blue, or green.

The experiment consisted of 8 functional runs, each lasting about 7 minutes. There were a total of 384 trials, 48 per run. Optimal sequencing software (OptSeq2, https://surfer.nmr.mgh.harvard.edu/optseq/) was employed to determine the variable duration of the jitter fixation (0-6200ms) and the order of trial types in each of the conditions within each

functional run to optimize efficient recovery of the blood-oxygen level dependent (BOLD) response (Dale 1999).

Before entering the scanner, participants were shown the response pads and were asked to practice on some trials to ensure they had understood the instructions correctly. Inside the scanner, before acquiring functional data, the size of the string of characters was manipulated during a set of titration blocks to ensure each individual participant averaged about 70% hits. During the actual functional runs, the string of characters could vary between five possible sizes, starting with an intermediate size (7.55x1.75º). Accuracy was automatically calculated after each titration block (14 trials). If accuracy was above 78%, a smaller size (6.75x1.50º) was used during the next titration block. If accuracy was below 62%, the size was increased (8.22x1.90º) during the next titration block. The titration procedure ended when the participant completed two consecutive blocks in which the accuracy was in the range of >62% and <78%.

fMRI Data Acquisition

Functional and structural images were collected on a 3-T Siemens PRISMA Fit whole-body MRI scanner at the Mind, Brain, and Behavior Research Center (CIMCYC, University of Granada), using a 32-channel whole-head coil. Functional images were acquired in 8 separate functional runs using a gradient-echo echo-planar pulse sequence with the following acquisition parameters: time-to-repetition (TR) = 1550 ms, time-to-echo (TE) = 35 ms, 60 interleaved 2.4-mm cubic axial slides, no inter-slice gap, flip angle = 70°, field of view (FoV) = 210 mm, 275 volumes per run. Each functional run was preceded by four functional dummy scans to allow for T1-equilibration effects, which were discarded. High-resolution MPRAGE T1-weighted structural images were also collected for each participant with the following parameters: TR = 2530 ms, TE = 2.36 ms, flip angle = 7°, FoV = 256 mm, voxel resolution = 1 mm3, 176 slices.

fMRI Data Analysis

SPM12 (Wellcome Centre for Human Neuroimaging, London) was used to conduct standard preprocessing routines and analyses. Images were corrected for differences in slice acquisition timing and realigned to the first volume by means of rigid-body transformation. Motion parameters extracted from the realignment were used, after a partial spatial smoothing of 4-mm full width at half maximum (FWHM) isotropic Gaussian kernel, to inform additional motion correction algorithms implemented by the Artifact Repair toolbox (ArtRepair; Stanford Psychiatric Neuroimaging Laboratory). This allowed us to repair outlier volumes with sudden scan-to-scan motion exceeding 0.5 mm and/or 1.3% variation in global intensity and to correct these outlier volumes via linear interpolation between the nearest non-outlier time points (Mazaika et al. 2009). To further limit the influence of motion on our fMRI results, participants with more than 12% to-be-corrected outlier volumes across functional runs were excluded. Before applying this additional motion correction procedure, we also checked for participants who showed a drift over 3 mm/degrees in any of the translation (x, y, z) and rotation (yaw, pitch, roll) directions within each functional run. As a result of applying these motion correction criteria, we excluded a total of three participants from further data analyses.

After volume repair, structural and functional volumes were coregistered and spatially normalized to T1 and echo-planar imaging templates, respectively. The normalization algorithm used a 12-parameter affine transformation together with a nonlinear transformation involving cosine basis functions. During normalization, the volumes were sampled to 2-mm cubic voxels. Templates were based on the MNI305 stereotaxic space (Cocosco et al. 1997), an approximation of Talairach space (Talairach and Tournoux 1988). Then, functional volumes were spatially smoothed with a 7-mm FWHM isotropic Gaussian kernel. Finally, the time series were temporally filtered to eliminate contamination from the slow signal drift (high-pass filter: 128 s).

Statistical analyses were performed on individual participant's data using the general linear model (GLM). fMRI time series data were modeled by a series of events convolved with a canonical hemodynamic response function (HRF). We used a slow event-related model where the components of each trial (i.e., number, string of characters, central and peripheral tasks) were modeled together as a 6.2 s epoch, time-locked to their onset time. Trials were sorted as "far" or "near" based on the Central task condition (i.e., Central task factor), and as "hits" or "illusions" as a function of participants' responses to the peripheral task (i.e., Trial type factor). Thus, our main experimental design included 4 regressors for the 4 conditions of interest: far-hit, far-illusion, near-hit, and near-illusion. Errors on the central or peripheral tasks and unseen responses to the peripheral task were modeled separately and excluded from the main analysis. The motion parameters for translation (x, y, z) and rotation (yaw, pitch, roll) were also included as covariates of noninterest in this GLM. SPM12 FAST was used for temporal autocorrelation modeling in this GLM due to its optimal performance in terms of removing residual autocorrelated noise in first-level analyses (Olszowy et al. 2019). The least-squares parameter estimates of the height of the best-fitting canonical HRF for each condition were used in pairwise contrasts.

Contrast images, computed on a participant-by-participant basis, were submitted to group analysis. At the group level, whole-brain contrasts between conditions were computed by performing one-sample t-tests on these images, treating participants as a random effect. Family-wise error (FWE) correction at the cluster level, voxel-extent threshold of $p < .001$, was applied to whole-brain maps involving all participants. Given that one of the main objectives of the present study was to investigate differences in functional engagement for hits versus illusions, this contrast was computed at the whole-brain level to initially examine regions differentially recruited for these conditions. ROIs were created with the MARSBAR toolbox in SPM12 (Brett et al. 2002). ROIs consisted of significantly active voxels identified from the All > Null whole-brain functional contrast (cluster-wise FWE corrected, voxel-extent threshold of $p <.001$) across all participants within specific MARSBAR anatomical ROIs. A set of ROIs (the center of mass and the volume in mm^3 are indicated

between parentheses) previously related to attentional and feature integration processes (Leonards et al. 2000; Shafritz et al. 2002; Braet and Humphreys 2009; Gillebert and Humphreys 2010; Pollmann et al. 2014; Humphreys 2016), were built for time courses and functional connectivity analyses. These ROIs included the left angular gyrus (-30, -52, 34; 240 mm^3), right angular gyrus (29, -58, 46; 376 mm^3), left FEF (-23, -4, 58; 1712 mm^3), right FEF (25, -5, 62; 4808 mm^3), left inferior parietal lobe (IPL; -40, -41, 44; 9240 mm^3), right IPL (37, -43, 49; 2816 mm^3), left superior parietal lobe (SPL; -23, -58, 55; 7328 mm^3), right SPL (23, -57, 58; 6448 mm^3), left supramarginal gyrus (-56, -26, 29; 2896 mm^3), right supramarginal gyrus (50, -27, 34; 3128 mm^3). Since we had no different *a priori* hypothesis regarding the role of V1 and V2, occipital ROIs comprised a combination of V1 and V2 in the left (-10, -83, 2; 23432 mm^3) and right (12, -79, 4; 22792 mm^3) hemispheres.

For time course analyses, the BOLD activation time series, averaged across all voxels in each ROI, were extracted from each functional run. Mean time courses for each trial were then constructed by averaging together appropriate trial time courses, which were defined as 15.5-secs (10 TRs) windows of activation after trial onset. These condition-based time courses were then averaged across functional sessions and across participants. These data were then analyzed using repeated-measures ANOVAs with the factors Hemisphere (left vs. right), Trial type (hit vs. illusion), Central task condition (far vs. near), and Time (including 8 time points), with the main objective of examining functional temporal modulations, such as early versus late effects within epochs/trials.

Finally, we examined functional connectivity via the beta-series correlation method (Rissman et al. 2004) implemented in SPM12 with custom MATLAB scripts. The canonical HRF in SPM was fit to each trial from each experimental condition and the resulting parameter estimates (i.e., beta values) were sorted according to the study conditions of interest (Central task and Trial type) to produce a condition-specific beta series for each voxel. Three different functional connectivity analyses were performed: 1) pairwise functional connectivity between visual regions and the remaining ROIs using the main GLM and event durations (i.e., 6.2 s epochs); 2) pairwise functional

connectivity between visual regions and the rest of the ROIs based on two modified GLMs corresponding to the earlier time window of 3.1 s (i.e., Time window I) and the later time window of 3.1 s (i.e., Time window II); and 3) whole-brain functional connectivity for hits and illusions using left and right visual areas as seed regions.

For both pairwise functional connectivity analyses, we first calculated beta-series correlation values for each pair of ROIs at the participant level. Then, based on the Pearson r-values obtained for each pair of ROIs with visual cortex, we calculated the corresponding p-values. Next, we examined interactions in pairwise functional connectivity between these ROIs. Because correlation coefficients are inherently restricted to range from − 1 to + 1, an archyperbolic tangent transform was applied to these beta-series correlation r-values to make the null hypothesis sampling distribution approach that of the normal distribution (Fisher 1922). These Fisher's z normally distributed values were then submitted to repeated-measures ANOVAs with the factors Central task and Trial type. The temporal window factor Time window (I, II) was added to the second pairwise connectivity analyses to capture differences in functional coupling effects, during early and later stages of trial processing.

For the whole-brain functional connectivity analysis, the beta series associated with the visual areas were correlated with voxels across the entire brain to produce beta-correlation images separately for hits and illusions. Contrasts between beta-correlation images were also subjected to an archyperbolic tangent transform to allow for statistical inference based on temporally coupled fluctuations with this region. Hits > Null and illusions > Null one-sample t-tests were performed on the resulting subject contrast images to produce group correlation contrast maps with a threshold of $p < .05$ (cluster-wise FWE corrected).

Statistical analyses were performed with JASP (Team JASP 2019). Since the assumption of sphericity was violated in the time course analyses (indicated by Mauchly's test of sphericity), Greenhouse-Geisser correction was applied as implemented in JASP. In the ANOVAs of time course and functional connectivity analyses, post-hoc Bonferroni corrected comparisons were employed to

explore significant interactions. Data is available on https://osf.io/d8hj7/?view_only=5ec9b79f1d3c4120a571fdde5310e7e2. Note that in some analyses, missing cells indicate participants that were automatically removed.

Results

Behavioral Results

We were interested in two important behavioral results. First, we wanted to explore whether the proportion of hits, illusions, errors, and unseen responses in the peripheral task was modulated by central task demands. Since the distribution of these responses deviated from normality, Wilcoxon signed-rank tests were used to compare the mean proportion of hits, illusions, errors, and unseen responses for the two conditions in the Central task (far and near). Second, we wanted to explore whether responses to the central task demonstrated the expected pattern of results (slower responses for numbers closer to the standard), and if these responses were affected by responses to the peripheral task (hits and illusions; errors and unseen responses are not considered here since they were rare). For the central task, both accuracy and RT were emphasized. Both dependent variables were analyzed using repeated measure analysis of variance (ANOVAs) with the factors Central task condition (far and near) and Trial type (hits and illusions). The Wilcoxon W-statistic and the rank-biserial correlation (r_B), representing the effect size, are reported. Values <.1 are considered trivial, values around 0.1 are interpreted as a small effect, around 0.3 as a medium effect, and >0.5 as a large effect (Cohen 1992; Fritz et al. 2012; Goss-Sampson 2020).

The proportion of hits ($\bar{x}$ = .627 in the far condition and $\bar{x}$ = .625 in the near condition; W = 233.500, p = .413, r_B = .183), illusions ($\bar{x}$ = .298 for far and $\bar{x}$ = .291 for near; W = 188.000, p = .760, r_B = .071), errors ($\bar{x}$ = .050 for far and $\bar{x}$ = .054 for near; W = 131.500, p = .606, r_B = -.123), and unseen responses ($\bar{x}$ = .022 for far and $\bar{x}$ = .028 for near; W = 44.000, p = .129, r_B = -.425), was not significantly different across the two central task conditions (Figure 2A).

For the central task, RT analyses showed both a main effect of Central task condition, F(1, 27) = 83.107, p < .001, η^2_p = .755, and a main effect of Trial type, F(1, 27) = 15.014, p < .001, η^2_p = .357, indicating that participants' responses were faster in the far as compared to the near condition, and in those trials in which participants responded correctly to the peripheral task (hits) as compared to illusions (Figure 2B). Participants accurately responded to the central task ($\bar{x}$ = .970); in the accuracy analysis, only a main effect of Central task condition was found, F(1, 27) = 19.871, p < .001, η^2_p = .424, with more accurate responses for far ($\bar{x}$ = .983) than near ($\bar{x}$ = .965) conditions.

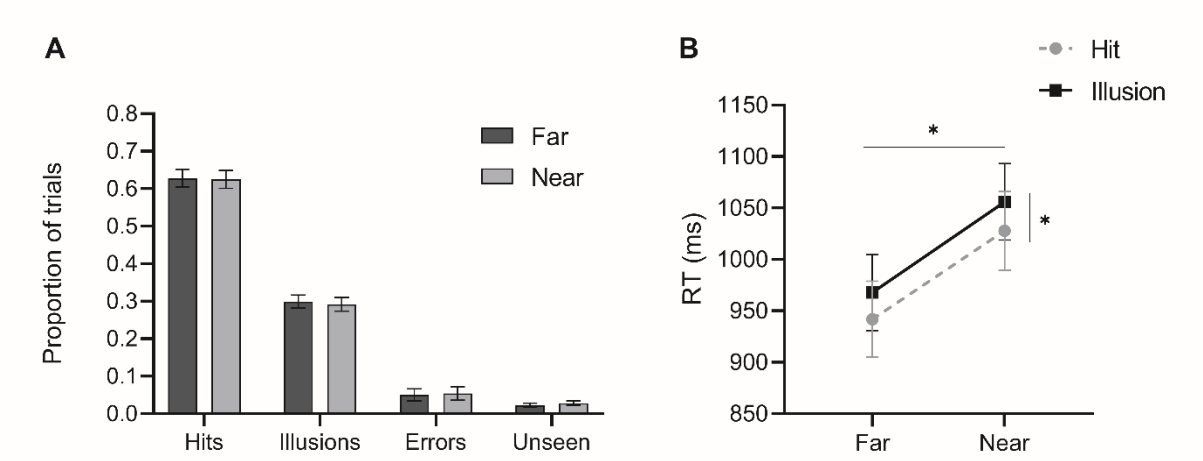

Figure 2. Behavioral task results. **A)** Proportion of hits, illusions, errors, and unseen responses for each Central task condition (far and near). The figure shows that the Central task did not modulate participants' responses. **B)** RT for the central task as a function of Central task condition (far and near) and Trial type (hit and illusion). The figure shows a main effect of Central task and a main effect of Trial type. Asterisks represent statistically significant comparisons. Error bars represent standard errors.

In sum, results from the peripheral task showed that the manipulation was successful in producing an average mean of 30% illusory conjunctions. Even though we found no differences in the proportion of hits and illusions between the two Central task conditions, which indicates that the Central task was not effectively interfering with perceptual reports in the peripheral task, responses were faster in the far as compared to the near condition. Moreover, although participants did not respond to the peripheral task until later in the trial, RT for the Central task was faster when a hit rather than an illusion occurred later. This result has been previously and consistently observed

(Cobos and Chica 2022). It might be due to a preparatory process that modulates performance, even if the demands of the Central task did not directly modulate the number of illusions produced in the peripheral task.

fMRI Results

The main aim of the fMRI analysis was to compare brain activations and co-activations for hits and illusions. The whole-brain contrast hits vs. illusions showed larger BOLD responses for hits than illusions in a set of brain regions comprising frontal, parietal, and occipital areas (Figure 3). The whole-brain contrast near vs. far (cluster-wise FWE corrected, $p < .001$ voxel extent) did not reveal any significant activations above threshold.

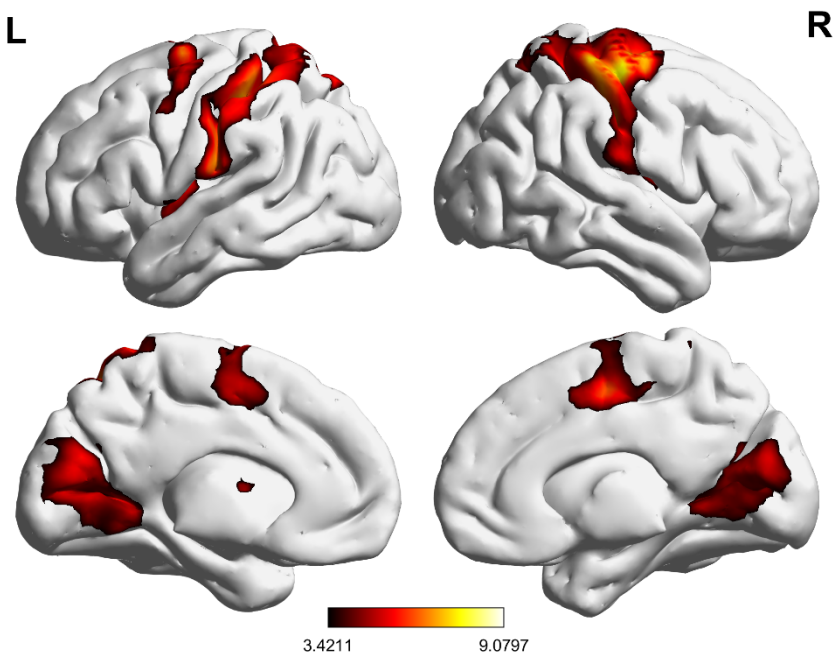

Figure 3. Whole-brain hits > illusions contrast showing brain areas with larger BOLD responses for hits than illusions (cluster-wise FWE corrected, $p < .001$ voxel extent). At the whole-brain level no brain region demonstrated increased responses for illusions vs. hits.

We then examined the time course analyses of the BOLD response to examine possible functional temporal modulations, such as early versus late effects within trials, for the regions of interest. Given the bilateral nature of the results and to reduce the number of comparisons,

hemisphere was included in the ANOVAs as a factor. Therefore, for each ROI, the ANOVA included the factors Trial Type (hit vs. illusion), Central Task condition (far vs. near), Hemisphere (left vs. right), and Time (8 time points). In V1-V2, we observed an interaction between Trial Type and Time, $F(1, 27) = 7.628$, $p < .001$, $\eta^2_p = .220$, with larger BOLD signal intensity for illusions as compared to hits at early time points (with a significant difference at 3.10 sec., $p_{Bonf} = .004$, and 4.65 sec., $p_{Bonf} = .001$); all other comparisons between hits and illusions at the remaining time points were not significant, $p_{Bonf} \geq .026$ (see Figure 4).

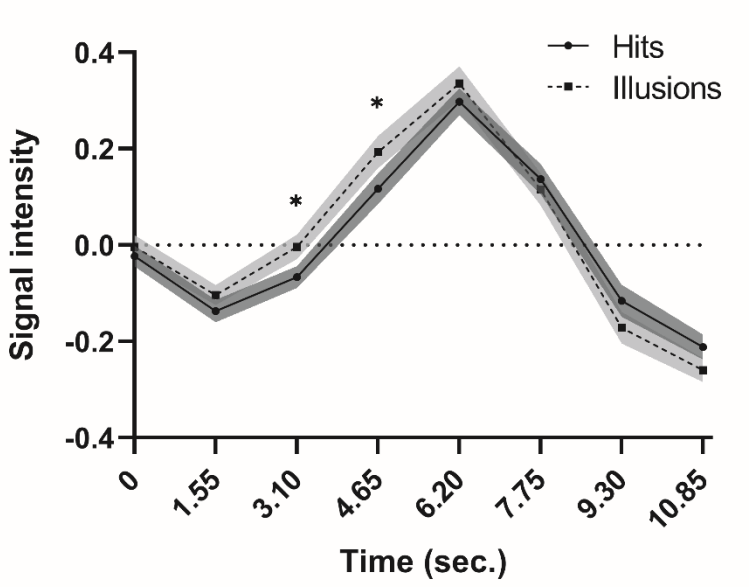

Figure 4. Time courses for V1-V2 showing increased BOLD signal intensity for illusions (light gray, dashed line) than hits (dark gray, solid line) at early time points (3.10 and 4.65 sec.). Asterisks represent significant comparisons for hits vs. illusions at each time point (Bonferroni corrected). Error envelopes represent standard errors.

We also found a significant interaction between Central task, Trial type and Time in the FEF, $F(1, 27) = 3.849$, $p = .017$, $\eta^2_p = .125$ (the interaction with hemifield was not significant). However, post-hoc comparisons at different time points in each condition were not significant (all $ps_{Bonf} \geq .035$).

Since V1-V2 was the only area showing the Trial type by Time interaction at the regional level, with increased activation for illusions as compared to hits at early intervals, we conducted two different functional connectivity analyses to further examine if these areas showed differential connectivity patterns for hits and illusions. First, pairwise functional connectivity among visual regions and the rest of the ROIs was analyzed using the original GLM model with 6.2 s per epoch. We ran a repeated measure ANOVAs on the Fisher's z values of each pair of regions obtained in this analysis (with the factors Central task and Trial type). Figure 5A represents the pairs of regions that showed a significant main effect of Trial type, with all the statistically significant pairs showing stronger functional coupling for hits than illusions (all Fs (1, 26) ≥ 5.977, all ps ≤ .022, all $\eta^2_{ps} \geq .187$). Second, a similar functional connectivity analysis focused on pairwise connections between left and right V1-V2 with the remaining ROIs being conducted by dividing the original GLM model with 6.2 s epochs into two modified GLMs corresponding to the earlier time window of 3.1 s (i.e., Time window I) and the later time window of 3.1 s (i.e., Time window II) to examine potential time-varying effects in functional coupling effects for hits and illusions during the earlier and later stages of the trials. The Fisher's z values for each pair of regions with left and right V1-V2 derived from this analysis were also submitted to the same type of repeated measures ANOVAs as previous analyses, adding the factor Time window (I, II). This analysis revealed an interaction in right V1-V2 and right FEF between Trial type and Time window, $F(1, 27) = 5.785$, $p = .023$, $\eta^2_p = .176$, which showed comparable functional coupling for hits and illusions in the early time window, $p_{Bonf} = 1.000$, but increased coupling for hits compared to illusions in the later time window, $p_{Bonf} = .003$ (see Figure 5B and 5C).

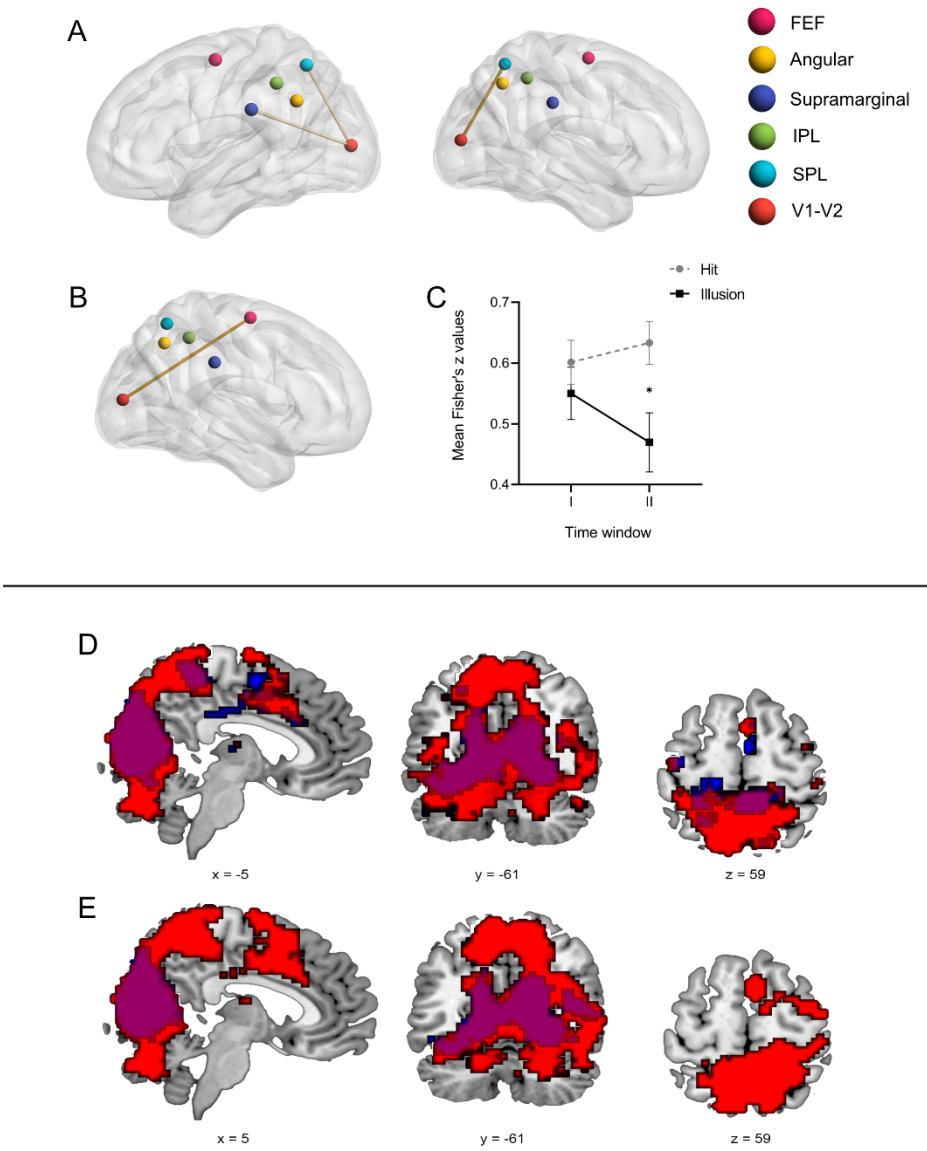

Figure 5. Representations for both types of functional connectivity analyses, pairwise (top panel) and whole-brain (bottom panel). **A** Pairwise functional connectivity between ROIs showing a main effect of Trial type. Edges indicate statistically significant increases in functional connectivity between pairs of regions for hits compared to illusions. **B** Pairwise functional connectivity between the right V1-V2 and right FEF showing a significant Trial type by Time interaction. **C** Line graph showing Fisher's Z values for the Trial type by Time interaction in the functional coactivation between V1-V2 and FEF in the right hemisphere. Asterisks represent significant comparisons for hits and illusions. Error bars represent standard errors. **D-E** Whole-brain functional

connectivity using left (**D**) and right (**E**) V1-V2 as seeds for the contrasts (cluster-wise FWE corrected, $p < .001$ voxel extent) hits > null (red), illusions > null (blue), and overlap of the two (purple).

Finally, additional whole-brain functional connectivity analyses separately for hits and illusions were performed using seeds placed in the left and right V1-V2 using the original GLM model with 6.2 s epochs to conduct this beta-series connectivity analysis. The analysis was performed to ensure we had not missed potentially relevant co-activations between V1-V2 and the rest of the brain in the previous ROI-based pairwise connectivity analysis for each of the main conditions of interest. We found that while both illusions and hits involved co-activation between V1-V2 and other regions within the occipital cortex, hits showed additional functional coupling with the parietal lobe (Figure 5D and 5E).

Discussion

Visual features such as color, shape, orientation, size, etc., are processed in specialized brain regions, but these features need to be combined to construct a single percept at a later stage. Even though this "problem" was partially solved by the discovery of groups of neurons that –in early stages– process more than a single feature (for example, V1 neurons process both movement and orientation; (Tootell et al. 1998; Shu et al. 2015; Groen et al. 2017), the computational issue remains unsolved, since additional features may characterize the perceived object.

To better understand the brain mechanisms governing feature integration, this study used 1) a feature integration task which calibrated task difficulty to produce around 30% illusory conjunctions in each participant, and 2) a number comparison task to examine divided attention in feature binding. Behaviorally, the attentional demands of the central number task did not modulate the percentage of illusory conjunctions produced, although responses to the central task were slower when an illusion (as compared to a hit) occurred later in the trial. Elsewhere, we have suggested this effect could be due to preparatory processing, probably related to alerting

mechanisms, which affects responses to both the central task and the peripheral task (Cobos and Chica 2022), without directly affecting feature integration.

fMRI results demonstrated a distributed set of occipito-parieto-frontal areas with increased BOLD responses for correct feature binding (i.e., hits) compared to trials in which integration failed (i.e., illusions). Functional connectivity analyses demonstrated that V1-V2 were more strongly coupled with the parietal cortex for hits than illusions. This confirms the important role of the parietal lobe in feature integration (Shafritz et al. 2002). This role is likely related to establishing priority maps, which take both bottom-up stimulus salience and top-down behavioral priorities into account (Bisley and Goldberg 2010; Ptak 2012). Time-course analyses demonstrated larger BOLD signal intensity in V1-V2 at early time points for illusions versus hits. At early stages of processing, functional connectivity of primary visual areas with the FEF was comparable for hits and illusions; only at later intervals did functional connectivity between these regions increase for hits relative to illusions. Overall, these results demonstrated that hits are characterized by larger overall activation of occipito-parieto-frontal areas together with increased functional connectivity between occipital and parietal brain regions. On the other hand, illusory conjunctions are characterized by increased activation of occipital areas at early time points (as shown in the time-course analyses), decreased co-activation of right V1-V2 and the right FEF at later stages, and lower functional connectivity with the parietal cortex.

This functional characterization of brain activation and connectivity associated with correct and incorrect feature integration can provide evidence in favor of the FIT or the FCA. According to the FIT, attentional amplification from the parietal cortex should increase occipital responses for correct responses as compared to illusory conjunctions (Spitzer et al. 1988; Kastner et al. 1999). This was observed in the whole brain and ROI analyses, which demonstrated increased BOLD response for hits than illusions in occipital regions. However, the modulation of visual regions was time sensitive, and visual responses were increased for illusions than hits at early intervals. The FCA

proposes a two-stage account of feature integration, with an initial bottom-up stage of feature integration based on the activation of neurons sensitive to conjunctions of visual features. This process is fast, giving rise to rapid and confident responses, which are not supervised by the parietal cortex (according to Humphreys 2016; see also Humphreys 2001). After some time, a slower process starts, in which the results of the initial stage are confirmed through top-down feedback. This slow confirmation process is thought to be supported by the parietal cortex (Humphreys 2001, 2016; Gillebert and Humphreys 2010). The results from the time-course analyses seem consistent with this two-stage account, in which occipital areas are more active for illusions than hits at the fast-initial stage (as shown in the time-course analyses). However, with the time resolution of fMRI, the parietal cortex is more strongly connected to the occipital cortex both at initial and later stages, while it is the FEF that demonstrates increased functional connectivity for hits than illusions at the later stages but not at the initial stages. However, given the low temporal resolution of fMRI, our data do not disconfirm the assumption that the parietal cortex might not be properly coupled with occipital regions during the early stages of visual perception in the millisecond-scale (Braet and Humphreys 2009).

The FCA, supported by our results, is also in line with Moshe Bar's (2003) model of top-down facilitation in visual object recognition, in which low spatial frequencies from images are rapidly sent from early visual areas to frontal regions such as the ventrolateral and orbital prefrontal cortex. These rough representations activate predictions about the possible identity of the perceived object, which are then transmitted to the inferior temporal cortex. Similar proposals have aimed to explain how expectancy shapes perception (Seriès and Seitz 2013) through a circuit encompassing occipital, temporal, and ventral medial frontal cortex (Summerfield and Egner 2009). In a face completion paradigm, Chen and collaborators (2010) found that perceptual grouping of face fragments into a coherent face increased activity in high-level visual areas but decreased activity in early visual areas. This result is consistent with predictive coding models, suggesting that feedback from higher areas operates to reduce activation in lower areas. Our proposal is that all these perceptual processes (i.e.,

feature binding, perception of expected vs. unexpected objects, object completion) might use a similar mechanism, in which higher order areas (parietal and FEF regions in our study) send feedback to visual areas, reducing activation when perception is successful. This mechanism differs from attention, which increases activation in visual areas when objects are attended (Spitzer et al. 1988; Kastner et al. 1999).

Contrary to previous proposals (Treisman and Gelade 1980), prior results have demonstrated that visual conjunctions of features are represented in early visual areas such as V1 (Seymour et al. 2009, 2010). However, the authors acknowledge that their results do not unequivocally demonstrate that feature binding occurs in this region. The V1 fMRI response could therefore reflect the binding of information taking place in this area, but also feedback from the fronto-parietal network regarding already bound information (Whitney 2009). Our results suggest the importance of parietal regions and the FEF in top-down feedback to early visual regions, in line with studies showing that functional connection between the FEF and visual regions is relevant for top-down control of visual information (Bressler et al. 2008; Wang et al. 2016; Veniero et al. 2021). These results also indicate that, alongside the well-known role of the parietal lobe in feature integration (Shafritz et al. 2002), top-down feedback from the FEF might support correct feature integration. The FEF can influence the activation of neurons in the extrastriate cortex (Silvanto et al. 2006), improving perceptual processes (Grosbras and Paus 2003). The FEF also contains topographically organized saliency maps (Thompson and Bichot 2005; Vernet et al. 2014), which could support feature-binding for objects presented in different spatial locations. Failures in top-down FEF control have been related to incorrect integration of features, demonstrating that other regions of the dorsal fronto-parietal network (Corbetta 1998) besides the parietal cortex play a role in correct feature integration.

Interestingly, feature integration can occur even when stimuli are not consciously processed. Fahrenfort et al. (2017) trained classifiers to distinguish between Kanizsa figures (whose elements

are perceptually integrated to result in surface perception) and control figures, in which such integration does not occur. They compared the perception of these figures in conscious and unconscious conditions with an *Attentional Blink* paradigm, and in masking or non-masking conditions. Results demonstrated that the classifiers could not distinguish between Kanizsa and control figures when targets were masked, indicating that masking alters feature integration. However, the classifier was able to distinguish between Kanizsa figures and control figures, despite the fact that participants did not perceive the stimuli due to the *Attentional Blink*. This suggests that feature integration precedes, and is independent of, conscious perception. In our case, targets were always visible, but the stimulation was adjusted so that feature integration failed in a percentage of trials. Even though we used a mask in our design (which is believed to affect locally recurrent interactions and not feedforward processing, Fahrenfort et al. 2017), the mask is present in all conditions, both when the features were successfully integrated and when integration was incorrect. Incorrect feature integration in the present experimental conditions with supra-threshold information was therefore associated with failures in recurrent interaction processes between parieto-frontal and occipital structures, as observed in Fahrenfort et al.'s *Attentional Blink* manipulation.

In relation to the manipulation of divided attention with the central task, although attentional demands from this task did not modulate the proportion of illusions experienced, the dual task used in this study was effective in producing larger RTs for the more demanding (near) as compared to the less demanding (far) condition. fMRI results overall demonstrated no main effects of Central Task. There was only a significant interaction between Central Task, Trial Type, and Time in the FEFs. However, this interaction is difficult to interpret as post-hoc comparisons were not significant. In general, the absence of interactions between Central Task and Trial Type indicates different brain regions should be involved in either task. However, this result should be interpreted with caution given that no brain modulations were observed for the two difficulty conditions of the central task.

Limitations

An intrinsic limitation of fMRI is its poor temporal resolution. We used sensitive time-course analyses and examined functional connectivity across two consecutive time windows, but future research should explore functional correlates associated with correct and incorrect feature integration using even more time sensitive techniques. Even though the increased activation for illusions than hits at early time points showed in the time course analysis is an interesting result in line with the theoretical frames discussed in this paper, it was an unexpected result that should be replicated in future studies. Another limitation of our analysis is the fact that our data do not indicate the directionality of information flow. The sluggishness of the BOLD signal may prevent precise exploration of the directionality of information processing between occipital, parietal, and frontal areas, but future studies using Dynamic Causal Modeling analyses may be able to shed further light on the role of forward and feedforward processing in feature integration. Further research could also employ new methods, such as multivariate pattern analyses to explore how information is represented in different brain regions when correct and incorrect feature integration takes place. However, our study was not designed with the aim of applying these techniques, which requires a series of methodological considerations (O'Toole et al. 2007; Weaverdyck et al. 2020).

A further limitation refers to whether the illusory conjunctions observed in the present experiment are related to pure perceptual processes or if they are influenced by memory processes, especially because in this task, participants first respond to the central task, and then report the color of the peripherally presented target. The role of the parietal cortex in feature integration and also in working memory (Mackey et al. 2016; MacKey and Curtis 2017) supports the possibility that errors in feature integration in this experiment might be related to perceptual processes, memory processes, or a combination of both.

Conclusions

Our results demonstrate the critical role of the parietal cortex in feature integration. While correct feature integration was associated with overall activation of occipito-parieto-frontal areas together with increased occipito-parietal functional connectivity, incorrect feature integration was characterized by increased activation of occipital areas at early stages of processing together with decreased occipito-parietal and occipito-frontal coactivation. These results are consistent with the FCA, which acknowledges the importance of top-down feedback in the formation of stable perceptual representations.

References

Bar M. 2003. A Cortical Mechanism for Triggering Top-Down Facilitation in Visual Object Recognition. Journal of Cognitive Neuroscience. 15:600–609.

Baumgartner F, Hanke M, Geringswald F, Zinke W, Speck O, Pollmann S. 2013. Evidence for feature binding in the superior parietal lobule. NeuroImage. 68:173–180.

Bernstein LJ, Robertson LC. 1998. Illusory Conjunctions of Color and Motion With Shape Following Bilateral Parietal Lesions. Psychological Science. 9:167–175.

Bisley JW, Goldberg ME. 2010. Attention, Intention, and Priority in the Parietal Lobe. http://dx.doi.org/101146/annurev-neuro-060909-152823. 33:1–21.

Block N. 1995. On a confusion about a function of consciousness. Behavioral and Brain Sciences. 227–287.

Block N. 2005. Two neural correlates of consciousness. Trends in cognitive sciences. 9:46–52.

Block N. 2011. Perceptual consciousness overflows cognitive access. Trends in Cognitive Sciences. 15:567–575.

Braet W, Humphreys GW. 2009. The role of reentrant processes in feature binding: Evidence from neuropsychology and TMS on late onset illusory conjunctions. Visual Cognition. 17:25–47.

Bressler SL, Tang W, Sylvester CM, Shulman GL, Corbetta M. 2008. Top-Down Control of Human Visual Cortex by Frontal and Parietal Cortex in Anticipatory Visual Spatial Attention. Journal of Neuroscience. 28:10056–10061.

Brett M, Anton J-L, Valabregue R, Poline J-B. 2002. Region of interest analysis using an SPM toolbox [abstract]. NeuroImage. 16.

Chen J, Zhou T, Yang H, Fang F. 2010. Cortical Dynamics Underlying Face Completion in Human Visual System. Journal of Neuroscience. 30:16692–16698.

Chica AB, Bartolomeo P. 2012. Attentional Routes to Conscious Perception. Frontiers in Psychology. 3.

Cobos MI, Chica AB. 2022. Attention does not always help: the role of expectancy, divided, and spatial attention on illusory conjunctions. Quarterly Journal of Experimental Psychology.

Cocosco C, Kollokian V, Kwan R, Evans AC. 1997. BrainWeb: Online interface to a 3D MRI simulated brain database. In: 3rd Int Conf Funct Mapp Hum Brain.

Cohen J. 1992. Statistical Power Analysis. Current Directions in Psychological Science. 1:98–101.

Corbetta M. 1998. Frontoparietal cortical networks for directing attention and the eye to visual locations: Identical, independent, or overlappingneural systems? Proc Natl Acad Sci USA. 95:831–838.

Dale AM. 1999. Optimal Experimental Design for Event-Related fMRI. Hum Brain Mapping. 8:109–114.

Donner T, Kettermann A, Diesch E, Ostendorf F, Villringer A, Brandt SA. 2000. Involvement of the human frontal eye field and multiple parietal areas in covert visual selection during conjunction search. European Journal of Neuroscience. 12:3407–3414.

Esterman M, Prinzmetal W, Robertson L. 2004. Categorization influences illusory conjunctions. Psychonomic Bulletin & Review. 11:681–686.

Esterman M, Verstynen T, Robertson LC. 2007. Attenuating illusory binding with TMS of the right parietal cortex. NeuroImage. 35:1247–1255.

Fahrenfort JJ, van Leeuwen J, Olivers CNL, Hogendoorn H. 2017. Perceptual integration without conscious access. 114.

Fiebelkorn IC, Kastner S. 2020. Functional Specialization in the Attention Network. Annual Review of Psychology. 71:221–249.

Fisher RA. 1922. On the mathematical foundations of theoretical statistics. Philosophical Transactions of the Royal Society of London Series A, Containing Papers of a Mathematical or Physical Character. 222:309–368.

Friedman-Hill, Robertson L, Treisman A. 1995. Parietal contributions to visual feature binding: evidence from a patient with bilateral lesions. Science. 269:853–855.

Fritz CO, Morris PE, Richler JJ. 2012. Effect size estimates: Current use, calculations, and interpretation. Journal of Experimental Psychology: General. 141:2–18.

Gillebert CR, Humphreys GW. 2010. The decomposition of visual binding over time: Neuropsychological evidence from illusory conjunctions after posterior parietal damage. Visual Cognition. 18:954–980.

Goss-Sampson M. 2020. Statistical analysis in JASP: A guide for students. JASP.

Groen IIA, Silson EH, Baker CI. 2017. Contributions of low- and high-level properties to neural processing of visual scenes in the human brain. Philosophical Transactions of the Royal Society B: Biological Sciences. 372:20160102.

Grosbras M-H, Paus T. 2003. Transcranial magnetic stimulation of the human frontal eye field facilitates visual awareness. European Journal of Neuroscience. 18:3121–3126.

Humphreys GW. 2001. A multi-stage account of binding in vision: Neuropsychological evidence. Visual Cognition. 8:381–410.

Humphreys GW. 2016. Feature Confirmation in Object Perception: Feature Integration Theory 26 Years on from the Treisman Bartlett Lecture. Quarterly Journal of Experimental Psychology. 69:1910–1940.

Hung J, Driver J, Walsh V. 2011. Visual Selection and the Human Frontal Eye Fields: Effects of Frontal Transcranial Magnetic Stimulation on Partial Report Analyzed by Bundesen's Theory of Visual Attention. Journal of Neuroscience. 31:15904–15913.

Kastner S, Pinsk MA, de Weerd P, Desimone R, Ungerleider LG. 1999. Increased Activity in Human Visual Cortex during Directed Attention in the Absence of Visual Stimulation. Neuron. 22:751–761.

Kastner S, Ungerleider LG. 2000. Mechanisms of Visual Attention in the Human Cortex. Annual Review of Neuroscience. 23:315–341.

Lamme VAF. 2006. Towards a true neural stance on consciousness. Trends in cognitive sciences. 10:494–501.

Lamme VAF. 2010. How neuroscience will change our view on consciousness. Cognitive neuroscience. 1:204–220.

Leonards U, Sunaert S, van Hecke P, Orban GA. 2000. Attention Mechanisms in Visual Search - An fMRI Study. Journal of Cognitive Neuroscience. 12:61–75.

Li Z. 2002. A saliency map in primary visual cortex. Trends in cognitive sciences. 6:9–16.

MacKey WE, Curtis CE. 2017. Distinct contributions by frontal and parietal cortices support working memory. Scientific Reports 2017 7:1. 7:1–7.

Mackey WE, Devinsky O, Doyle WK, Golfinos JG, Curtis CE. 2016. Human parietal cortex lesions impact the precision of spatial working memory. J Neurophysiol. 116:1049–1054.

Mazaika PK, Hoeft F, Glover GH, Reiss AL. 2009. Methods and Software for fMRI Analysis of Clinical Subjects. NeuroImage. 47:S58.

Mudrik L, Faivre N, Koch C. 2014. Information integration without awareness. Trends in cognitive sciences. 18:488–496.

Olszowy W, Aston J, Rua C, Williams GB. 2019. Accurate autocorrelation modeling substantially improves fMRI reliability. Nature Communications. 10:1220.

O'Toole AJ, Jiang F, Abdi H, Pénard N, Dunlop JP, Parent MA. 2007. Theoretical, Statistical, and Practical Perspectives on Pattern-based Classification Approaches to the Analysis of Functional Neuroimaging Data. Journal of Cognitive Neuroscience. 19:1735–1752.

Pitts MA, Lutsyshyna LA, Hillyard SA. 2018. The relationship between attention and consciousness: An expanded taxonomy and implications for no-report paradigms. Philosophical Transactions of the Royal Society B: Biological Sciences. 373.

Pollmann S, Zinke W, Baumgartner F, Geringswald F, Hanke M. 2014. The right temporo-parietal junction contributes to visual feature binding. NeuroImage. 101:289–297.

Ptak R. 2012. The frontoparietal attention network of the human brain: Action, saliency, and a priority map of the environment. Neuroscientist. 18:502–515.

Ramkumar P, Lawlor PN, Glaser JI, Wood DK, Phillips AN, Segraves MA, Kording KP. 2016. Feature-based attention and spatial selection in frontal eye fields during natural scene search. Journal of Neurophysiology. 116:1328–1343.

Rissman J, Gazzaley A, D'Esposito M. 2004. Measuring functional connectivity during distinct stages of a cognitive task. NeuroImage. 752–763.

Robertson LC. 2003. Binding, spatial attention and perceptual awareness. Nature Reviews Neuroscience. 4:93–102.

Schneider W, Eschman A, Zuccolotto A. 2002. E-Prime 2.0. Pittsburgh: Psychology Software Tools, Inc.

Seriès P, Seitz AR. 2013. Learning what to expect (in visual perception). Frontiers in Human Neuroscience. 7.

Seymour K, Clifford CWG, Logothetis NK, Bartels A. 2009. The Coding of Color, Motion, and Their Conjunction in the Human Visual Cortex. Current Biology. 19:177–183.

Seymour K, Clifford CWG, Logothetis NK, Bartels A. 2010. Coding and Binding of Color and Form in Visual Cortex. Cerebral Cortex. 20:1946–1954.

Shafritz KM, Gore JC, Marois R. 2002. The role of the parietal cortex in visual feature binding. Proceedings of the National Academy of Sciences. 99:10917–10922.

Shu N, Gao Z, Chen X, Liu H. 2015. Computational Model of Primary Visual Cortex Combining Visual Attention for Action Recognition. PLOS ONE. 10:e0130569.

Silvanto J, Lavie N, Walsh V. 2006. Stimulation of the Human Frontal Eye Fields Modulates Sensitivity of Extrastriate Visual Cortex. Journal of Neurophysiology. 96:941–945.

Spitzer H, Desimone R, Moran J. 1988. Increased attention enhances both behavioral and neuronal performance. Science. 240:338–340.

Summerfield C, Egner T. 2009. Expectation (and attention) in visual cognition. Trends in Cognitive Sciences. 13:403–409.

Talairach J, Tournoux P. 1988. Co-planar stereotaxic atlas of the human brain: 3-dimensional proportional system: an approach to cerebral imaging. Stuttgart ; New York: Georg Thieme.

Team JASP. 2019. JASP, RRID:SCR_015823.

Thompson KG, Bichot NP. 2005. A visual salience map in the primate frontal eye field. In: Progress in Brain Research. Elsevier. p. 249–262.

Tootell RBH, Hadjikhani NK, Vanduffel W, Liu AK, Mendola JD, Sereno MI, Dale AM. 1998. Functional analysis of primary visual cortex (V1) in humans. Proceedings of the National Academy of Sciences. 95:811–817.

Treisman A. 1998. Feature binding, attention and object perception. PhilTrans R Soc Lond B. 1295–1306.

Treisman A, Gelade G. 1980. A Feature-Integration Theory of Attention. Cognitive Psychology. 97–136.

Treisman A, Schmidt H. 1982. Illusory Conjunctions in the Perception of Objects. Cognitive Psychology. 107–141.

Veniero D, Gross J, Morand S, Duecker F, Sack AT, Thut G. 2021. Top-down control of visual cortex by the frontal eye fields through oscillatory realignment. Nature Communications. 12:1757.

Vernet M, Quentin R, Chanes L, Mitsumasu A, Valero-CabrÃ© A. 2014. Frontal eye field, where art thou? Anatomy, function, and non-invasive manipulation of frontal regions involved in eye movements and associated cognitive operations. Frontiers in Integrative Neuroscience. 8.

Wang C, Rajagovindan R, Han S-M, Ding M. 2016. Top-Down Control of Visual Alpha Oscillations: Sources of Control Signals and Their Mechanisms of Action. Frontiers in Human Neuroscience. 10.

Weaverdyck ME, Lieberman MD, Parkinson C. 2020. Tools of the trade multivoxel pattern analysis in fMRI: A practical introduction for social and affective neuroscientists. Social Cognitive and Affective Neuroscience. 15:487–509.

Whitney D. 2009. Neuroscience: Toward Unbinding the Binding Problem. Current Biology. 19:R251–R253.

Acknowledgments

This work was supported by the Spanish Ministry of Science and Innovation research projects PSI2017-88136 and PID2020-119033GB-I00 and the local government of Andalusia (Proyectos de I+D+i en el marco del Programa Operativo FEDER, B-SEJ-570-UGR20) to Ana B. Chica. Pedro M. Paz-Alonso was supported by grants from the Spanish Ministry of Science and Innovation [RYC-2014-15440 and PGC2018-093408-B-I00], Neuroscience projects from the Fundación Tatiana Pérez de Guzmán el Bueno, Basque Government [PIBA-2021-1-0003], and a grant from "la Caixa" Banking Foundation under the project code LCF/PR/HR19/52160002. BCBL acknowledges support by the Basque Government through the BERC 2022-2025 program and by the Spanish State Research Agency through BCBL Severo Ochoa excellence accreditation CEX2020-001010-S.

Authorship Statement

Pablo Rodríguez San-Esteban: Investigation, Formal analysis, Writing - Original Draft.

Ana B. Chica: Conceptualization, Methodology, Writing - Review & Editing, Supervision, Funding acquisition.

Pedro M. Paz-Alonso: Formal analysis, Writing - Review & Editing, Supervision.